AIMS Energy, 13(5): 1133–1166.
DOI: 10.3934/energy.2025042
Received: 15 January 2025
Revised: 26 May 2025
Accepted: 04 September 2025
Published: 22 September 2025

https://www.aimspress.com/journal/energy

Research article

An improved mayfly optimization with modified perturb and observe based energy management in grid integrated renewable sources

Mahesh Palavalasa[1], Shamik Chatterjee[2], Sultan Ahmad[3,4,*], R.S.R. Krishnam Naidu[5], Krishan Arora[1], Hikmat A. M. Abdeljaber[6] and Jabeen Nazeer[3]

[1] School of Electronics and Electrical Engineering, Lovely Professional University, Punjab, India
[2] Department of Electrical, Electronics and Communication Engineering, GITAM School of Technology, GITAM Deemed to be University, Bangalore, India
[3] Department of Computer Science, College of Computer Engineering and Sciences, Prince Sattam Bin Abdulaziz University, Alkharj 11942, Saudi Arabia
[4] University Center for Research and Development (UCRD), Department of Computer Science and Engineering, Chandigarh University, Gharuan, Mohali 140413, Punjab, India
[5] Department of Electrical and Electronics Engineering, Nadimpalli Satyanarayana Raju Institute of Technology, Vishakhapatnam, India
[6] Department of Computer Science, Faculty of Information Technology, Applied Science Private University, Amman, Jordan

* **Correspondence:** Email: s.alisher@psau.edu.sa; Tel: +919661340744.

Abstract: Recent developments show that renewable energies would permanently, safely, and increasingly supply the world's energy needs. Even still, there are some differences in their findings due to climate change, which is a significant problem. To overcome this issue, the Energy Management System (EMS) is introduced to satisfy the demands needs and increase the efficiency of renewable energy to ensure the effectiveness in an optimal way. We implemented a new method of improved Mayfly Optimization based Modified Perturb and Observe (IMO-MP&O) to enhance battery use, ensure energy flow stabilization, and meet the energy needs of connected loads. The IMO-MP&O concept satisfies energy requirements, giving priority to important applications and adapting to fluctuating demands. The main innovation of IMO-MP&O is its adaptive optimization technique, which builds on the advantages of MO to improve the traditional MP&O algorithm. The suggested IMO-MP&O EMS prioritizes key loads, stabilizes energy flow, maximizes battery utilization, and adjusts to changing demands. The overall simulation outcomes display that suggested IMO-MP&O

outperforms other algorithms by injecting 5.386 kWh of energy into the grid, representing an enhancement in grid independence. The grid injection of 5.386 kWh is emphasized as a marker of improved grid independence through efficient utilization of surplus renewable generation after satisfying a fixed 35 kWh load. Further, in terms of computation time, the suggested IMO-MP&O attains a better value of 392.15 s than the Grey Wolf-Cuckoo Search Optimization.

Keywords: energy management system; grid integration; hybrid renewable energy sources; improved mayfly optimization; modified perturb and observe

1. Introduction

In recent years, energy sources in terms of attitude comprise solar, tidal, biomass, and wave energy. These are thought to be limitless since they constantly and repeatedly reproduce themselves [1,2]. In terms of these renewable resources, wind and solar power stand out. Because sunshine and wind are present globally, these components are being researched more completely than other renewable sources [3,4]. Since they are dependent on the working surroundings and energy requirements [5], all scattered resources are handled manually and in parallel in a distributed manner [6]. PV systems cannot produce electricity continuously once the sunlight is not rising. On the other side, if there is no wind, a wind farm will not function [7]. In this instance, the essential power must consume a system to make up for its nonappearance in the event that the network operates inconsistently or that the conjunction generates less power than is necessary [8,9]. Making sure the system works effectively and never runs out of electricity is made possible through power management [10]. The main goal is to acquire sustained voltage and frequency renewable energy that is reliable. There should be strict control over harmonic distortion during and after electricity production [11]. Green resources have been the only source boosting the capability of the world's power stations, as described in [12].

While costs have reduced, renewable energy technology efficiency has increased [13,14]. Despite the lack of sunlight or humid air, portable power packs must be kept charged. The equipment would not function without the requirement for a battery backup. As mentioned, combining environmentally friendly wind and solar energy sources increases global energy production [15]. Moreover, along with ensuring a steady supply of electricity, a battery storage system is developed to make up for any shortfalls in renewable energy. In contemporary studies, battery saving tools are commonly employed [16]. In order to lessen the impact of solar and wind power generation fluctuation on the grid, efficient power management techniques must be developed [17,18]. Battery storage systems are a common component of current solutions [19,20]; however, their dependability and efficiency can be compromised by non-linear construction, load side destabilization, and regulatory obligations [21,22]. With the rising integration of renewable energy sources such as solar and wind into modern power systems, ensuring a reliable and efficient energy supply has become a pressing challenge, particularly due to their intermittent nature. Current energy management systems often struggle with maintaining grid stability and meeting fluctuating demand without over-reliance on non-renewable backup systems. We are motivated by the need to develop a more intelligent and adaptive control strategy for hybrid energy systems. Therefore, we address the basic need for an ideal power management system that can ensure a consistent and reliable energy supply from renewable sources. Using the IMO-MP&O control technique, we aim to bridge the gap between the variability of solar and wind power supply and the

demand for high-quality power. On the other hand, the IMO technique is designed to use a factor of measurement in order to regulate its process and produce optimal results. Using MP&O helps address the drift problem that causes the extracted power to oscillate. The IMO-MP&O control that is being presented takes into account the non-linear architecture, load side destabilization, and regulating responsibilities on the load generator ends. Further, the suggested IMO-MP&O based EMS prioritizes key loads, stabilizes energy flow, maximizes battery utilization, improves grid independence, and reduces the computation time. The contributions to the study are listed as follows:

- In this study, IMO-MP&O adjusted step size and found the duty cycle necessary ratio. The IMO-MP&O EMS lessens grid overvoltage issues caused by high voltage from renewable sources in order to preserve a stable and secure grid.
- To meet the demands of a peak demand, IMO and MP&O create an efficient EMS. This research provides a robust and efficient power management technique that ensures a steady and reliable energy supply from solar and wind power sources through the use of IMO-MP&O.
- Consistent energy regulation from secondary stage sources is achieved by converter switching. Next, the MPPT voltage/current, Total Harmonic Distortion (THD), real/reactive power, grid voltage/current, and overall energy balance are used to evaluate the findings.

This research is organized as follows: In Section 2, we provide the literature review; in Sections 3 and 4, we elaborate the problem formulation and the objectives framed for this research; In Section 5, we demonstrate the modeling of renewable energy sources; In Section 6, we provide the proposed methodology and explain the mathematical equation for proposed IMO-MP&O algorithm; In Section 7, we demonstrate the result and its comparison; and in Section 8, we state the conclusion of this research.

2. Literature review

Saranya M. and Samuel GG [23] demonstrated an improved neural network grid to demonstrate an EMS in a hybrid PV-wind system. In these situations, the addition of an Energy Storage System (ESS) improves the microgrid's security and dependability. In this study, we examine energy management in a hybrid system that combines a wind energy system based on Permanent Magnet Synchronous Generators (PMSG) and PV sources. The Cuckoo search-assisted Radial Basis Function Neural Network (RBFNN) approach has been used as Maximum Power Point Tracking (MPPT) technology to track maximum PV power, and the PV output is improved with the assistance of a switching Trans-Quasi-Z-Source (TQZS) boost converter. With less power loss and settling time, the suggested method produces excellent power tracking efficiency. The converter power system requires another one additional capacitor to produce the energy balance between the sources.

El Mezdi K et al. [24] have shown how nonlinear control (NLC) design and EMS can increase the performance of a grid-connected wind-battery hybrid system. To attain balance in the energy distribution among the load and energy sources, the EMS creates energy flow scenarios. This balance seeks to improve electricity quality, guarantee DC-grid stability, and reduce overall system costs. There are two modes of operation: i) Adaptive power point tracking (PPT) mode, which takes demand-driven production and battery's state of charge (SOC) into account, and ii) $MPPT$ mode, which uses an optimization tool to maximize power extraction. The NLC-based EMS decreased system costs and performed well in management among load and energy sources. However, for a continuous power supply, NLC-based EMS techniques need a lot of maintenance.

A coordinated optimal operation of a grid-connected wind-solar microgrid including hybrid EMS was proposed by Abdelghany MB et al. [25]. Developing a comprehensive model predictive control method for a grid-connected wind and solar microgrid that incorporates a battery-ESS, a hydrogen-ESS, and communication with external users, such as battery/fuel cell electric vehicles, is our goal of this study. The control of the integrated system's energy production in both electric and hydrogen forms is necessary. The hybrid-ESSs' operational and economic costs, degrading problems, and the system's dynamic and physical limitations make up the suggested approach. The hybrid-ESSs' operational modes and the switches that connect them had to be modeled using the mixed-logic dynamic framework.

Using a meta-heuristic optimization approach, Grey Wolf with Cuckoo Search Optimization (GWCSO), Jasim AM et al. [26] showed how to size micro grid components optimally. This approach has been used to find the system's ideal component sizes, which result in the lowest levelized cost of energy and annual cost. To the best of knowledge, GWO and CS have never been combined to calculate the sizing of such system components for an islanded micro grid. The GWCSO analysis has been evaluated with CS, GWO, and ALO algorithms. Furthermore, a greater number of system component units were needed for the suggested maintain the computation time.

Reagan Molu RJJ et al. [27] EMS focused on optimization for uncertain grid-connected PV/battery microgrids. We concentrated on the effective operation of an ESS that was a component of a microgrid with solar integration. Resolving the new issues that emerge from the integration enables better energy management. A substantial chunk of this paper is dedicated to contrasting two independent EMS: The heuristic method and the linear programming strategy. The effectiveness and efficacy of these techniques in satisfying load needs are assessed. Consequently, the grid's running costs reach their maximum while maintaining an energy balance.

From the overall analysis, traditional energy management strategies are simple and easy to implement but often suffer from poor dynamic response and oscillations under rapidly changing load or weather conditions. Similarly, it proves that existing methods have the limitation of energy balance between the sources as well as computation time. These limitations motivate the use of an adaptive and self-tuning optimization technique, such as the proposed IMO-MP&O to address performance and stability challenges in hybrid renewable energy systems. Therefore, we suggest the IMO-MP&O optimization method, which uses Mayfly to improve MP&O, making it effective. This method prioritizes key loads, stabilizes energy flow, and maximizes battery utilization.

3. Problem formulation

Initially, the problem statements are looked at in this research in order to divide up electricity production between multiple sources for a grid-integrated technology. In order to maximize the overall restrictions, consumption and the electricity generating capacity are examined while determining the appropriate generation size using the multi-objective algorithm. The description about the load generation constraints is defined as follows.

3.1. Load generation constancy and limits

The key factor affecting the load's power usage being that prevents the creation of power (grid). The production of PV and wind energy is unclear since renewables are unpredictable and intermittent.

As a consequence, the battery's SOC (State of Charge) continues to be the article's main application. Equation (1) specifies the necessity of a grid power, which is monitored through distinct sources.

$$\sum_{k=1}^{N_k} P_{grid}(t) = \sum_{i=1}^{N_g} P_{Gi}(t) + \sum_{j=1}^{N_s} P_{Sj}(t)\, P_{Ej}(t) \tag{1}$$

P_{grid} is stated as the grid power. The quantity of grid is declared as $k, gands$. Total load is declared as N_k. P_{Ej} declares the storage allotted for production. P_{Gi} and P_{Sj} are signified as output power from wind and PV.

Equation (2) shows the lower and higher power production restrictions for each RES and battery storage component.

$$\begin{aligned} P_{Gi,min}(t) \leq\ & P_{Gi}(t) \leq P_{Gi,max}(t) \\ P_{Sj,min}(t) \leq\ & P_{Sj}(t) \leq P_{Sj,max}(t) \\ P_{Ej,min}(t) \leq & P_{Ej}(t) \leq P_{Ej,max}(t) \end{aligned} \tag{2}$$

Boundaries on charging and discharging levels of battery are represented in Eq (3).

$$SOC_{sj}(t) = SOC_{sj}(t-1) + P_{\frac{chg}{Dchg}}(t)$$

$$0 \leq \left| P_{\frac{chg}{Dchg}}(t) \right| \leq P_{CDsj,max} \tag{3}$$

$\mathrm{SOC_{sj}(t)}$ and $\mathrm{SOC_{sj}(t-1)}$ are the charging at current and previous times, respectively. $\mathrm{P_{\frac{chg}{Dchg}}(t)}$ is the charging/discharging throughout tth time, and $\mathrm{P_{CDsj,max}}$ is declared at maximum ranges. Consequently, the power fluctuation of a hybrid source is determined using a battery's SOC. Finding the right balance between excess electricity and energy densities is necessary for power dependence. It includes real-time power balancing under dynamic load situations, the intermittent nature of wind and solar energy sources, and the difficulty of preserving system stability and power quality while reducing dependency on non-renewable resources. The suggested IMO-MP&O approach is used because these difficulties necessitate a strong and flexible control strategy. Moreover, IMO-MP&O is exploited to define a fundamental problem for handling multi-objective issues.

4. Objectives

- During different loading scenarios, a hybrid technique is employed to assess the EMS of batteries and RES.
- To ascertain whether the hybrid solar-wind power system is capable of supporting the necessary load.
- A solution for optimizing the energy production and storage subsystems can be studied by combining more HES and examining the effects of load magnitude or characteristics.

5. Modeling of RES

5.1. PV

The p-n junction in the solar cells facilitates the conversion of solar energy into direct current power.

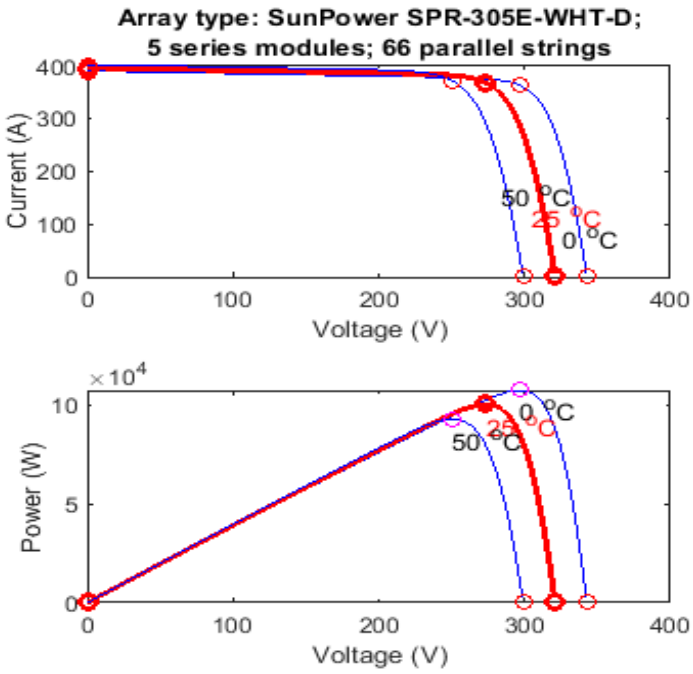

Figure 1. PV cell properties in V-I.

The analogous circuit of the PV model has two subtypes: Single diode and double diode. It is suggested that single diodes should be used for design and analytical research. Rising temperature, mode of operation field, and efficient factors are needed for all locations on PV power [28]. To calculate the voltage and solar capacity plane using the connection of module in solar parallel series, the MPPT technique is used by the solar array to increase the MPP. Figure 1 shows the cell of PV behavior in V-I. The considered PV array incorporates 10 SunPower SPR-305E-WHT-D modules, which yield a nominal array capacity of 3.05 kW at standard test conditions.

Equation (4) applied to monitor the power outcome,

$$P_{MPPT}(t) = I_{MPPT}(t) \times V_{MPPT}(t) \tag{4}$$

The present rate of voltage and current is defined in Eqs (5) & (6).

$$I_{MPPT}(t) = I_{SC}\left\{1 - C_1\left[exp\left(\frac{V_M}{C_2 \times V_{OC}}\right)\right]\right\} + \Delta I(t) \tag{5}$$

$$V_{MPPT}(t) = V_M + \mu V_{OC}.\Delta T(t) \tag{6}$$

V_{OC}&I_{SC} is signified as public voltage circuit and current short circuit; initial models are defined as C_1 & C_2; and V_M is represented as maximum voltage which are represented in Eqs (7)–(10) accordingly.

$$C_1 = \left(1 - \frac{I_M}{I_{SC}}\right) \times exp\left(-\frac{V_M}{C_2 \times V_{OC}}\right) \tag{7}$$

$$C_2 = \left(\frac{V_M}{V_{OC}} - 1\right) \times \left[ln\left(1 - \frac{I_M}{I_{SC}}\right)\right]^{-1} \tag{8}$$

$$\Delta I(t) = I_{SC}\left(\frac{GT(t)}{G_{ref}} - 1\right) + \alpha_{1,sc} \times \Delta T(t) \tag{9}$$

$$\Delta T(t) = T_c(t) - T_{c,ref} \tag{10}$$

I_M is stated as maximum current; $T_{c,ref}$ is stated as cell temperature; and $GT(t)$ is stated as the level of irradiation.

5.2. Wind energy

Height, volume, and velocity are the major determinants of generating capacity [29]. The major factors that determine wind model parameters are frequency and size. The wind screen indicates that the wind's velocity changes with altitude and does not remain constant. The Earth's climate is estimated to have an air velocity in 1000 meters of height per second with 14 meters. The wind turbine is modeled at a nominal speed of 9 m/s, with the output power computed from the standard turbine power curve. The wind subsystem is modeled as a Doubly-Fed Induction Generator (DFIG) turbine rated at a 50 kW. The aerodynamic power is computed using Eq (11).

$$P_{aero} = \frac{1}{2}\rho A C_p(\lambda, \beta) v^3 \tag{11}$$

where, ρ represents the density of air, A represents the rotor swept area, C_p is the power coefficient, and v is the wind speed. The current output follows the curve of turbine power and generator side control. Similarly, the instantaneous electrical power $P_w(t)$ is limited by the 50 kW turbine rating and accounts for generator and drivetrain efficiencies as implemented in DFIG block. Subsequently, Eq (12) shows the outcome of electrical wind while accounting for turbulent flow.

$$P_o = P_{rs}\begin{Bmatrix} 0 & V < V_{ci} \\ a \times V^3 - b \times P_{rs}, & V_{ci} < V < V_{rs} \\ 1 & V_{rs} < V < V_{cf} \end{Bmatrix} \tag{12}$$

P_o and P_{rs} are declared as output power and rated speed. The speed calculations of wind energy are stated in Eq (13).

$$V_{hub} = V_0 \times \left(\frac{Z_{hub}}{Z_0}\right) \times \alpha \tag{13}$$

Height is referred to as V_{hub}; reference speed is declared as V_0; actual height is referred as Z_{hub}; speed limit is characterized as Z_0; and α is stated as power.

5.3. Battery

The battery charges whenever the need for solar and wind-generated energy surpasses the supply [30]. Thus, the voltage of RES level states the discharge steps while in the extreme loads

$$SOC = SOC(t-1) \times (1-\sigma) + [P_{RES}(m) - P_L(t)/\eta_{inv}] \times \eta_{ch} \quad (14)$$

In the proposed hybrid EMS, the battery plays an important role in regulating energy balance by acting as a buffer among variable renewable generation and changing load demand. While periods of excess generation, when solar irradiance and wind speed yield power beyond the 50-kWh fixed load, the surplus energy is given to charge the battery until its State of Charge (SOC) obtains the upper threshold. PV modules contribute to charging during high irradiance hours (11:00–15:00), whereas wind power supplements charge in moderate-to-high wind speeds 9 m/s. In contrast, for low irradiance and calm wind conditions, the EMS controller activates battery discharging for meeting demand by maintaining grid stability. The discharge procedure is managed by SOC, which is restricted to prevent over-depletion by guaranteeing a continuous supply lacking damaging the battery. This coordinated charging/discharging mechanism helps in guaranteeing which renewable sources are utilized, grid dependence is decreased, and stable operation of hybrid system is preserved.

$$\mathrm{SOC} = \mathrm{SOC}(\mathrm{t}-1) \times (1-\sigma) + [\mathrm{P_L}(\mathrm{m})/\eta_{\mathrm{inv}} - \mathrm{P_{RES}}(\mathrm{t})] \times \eta_{\mathrm{disch}} \quad (15)$$

SOC and $\mathrm{SOC}(\mathrm{t}-1)$ declares the battery's charging and discharging in the Eqs (14) and (15). The outflow rate is declared as σ. $\mathrm{P_{RES}}$ and $\mathrm{P_L}$ denote from RES and load, respectively. η_{inv}, η_{ch}, and η_{disch} are significant according to the properties of charges. The explanation about the proposed methodology is described in the following section.

6. Proposed methodology

The integration of the IMO-MP&O method for real-time energy management in a hybrid renewable energy system is what makes this study novel. The suggested IMO-MP&O technique, in contrast to conventional EMS techniques, provides greater flexibility and quicker convergence, enabling more accurate power balance, lower THD, and better battery use. Under varying conditions, this optimization-control paradigm works especially well for controlling the dynamic behavior of grid-connected solar-wind systems.

The renewable energy forms energy and HRES by combining the sources of different electricity consumption forms. If renewable power stability is to be ensured, the present sources are also multifaceted. To guarantee reliability, the electricity sector needs to be rationalized, keeping in mind important elements, including economical price, friendly environment consequences, reliable mode work, and customer significance. The structure of the designed method is displayed in Figure 2. The design system is mainly used to evaluate data that is tested by the solar panel of MPPT system. It provides the necessary permutation for the key parameters. The management method lessens variations in grid frequency and voltage. The proposed controller regulates voltage power and chooses if the power was obtained or affected by a reactivation form in response to system fluctuations. The IMO-MP&O optimization method aims to achieve energy flow stabilization and manage the sources of secondary stage and converter switching difficulties in order to provide a dependable and efficient energy supply to linked loads while managing grid stability and compliance.

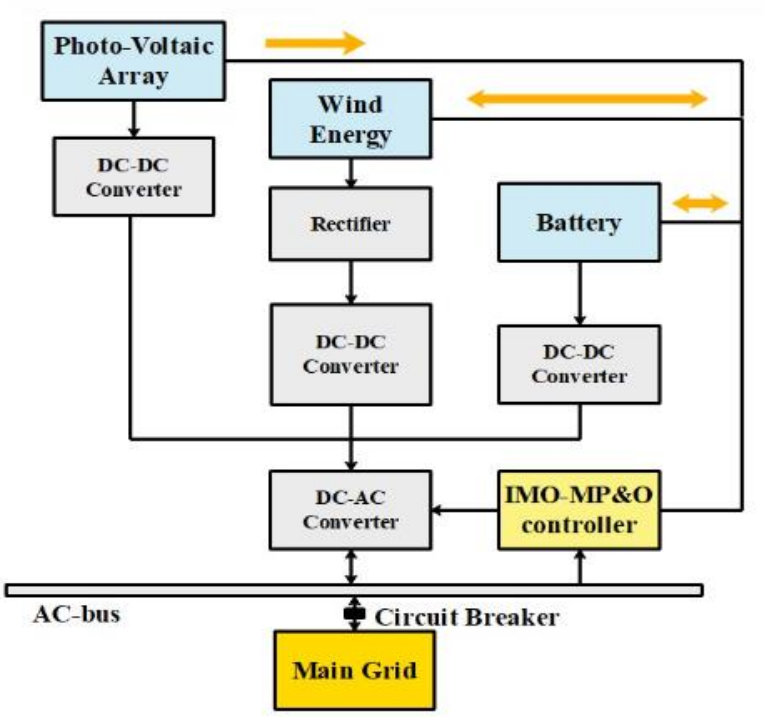

Figure 2. Block diagram.

6.1. Mayfly optimization

The IMO-IMP&O is chosen here because it successfully strikes a balance between exploration and exploitation. Moreover, this algorithm is selected to produce high-quality solutions and faster convergence in challenging, nonlinear energy management issues. It is especially well-suited for optimizing real-time control parameters in hybrid renewable systems because of its methodology, which is inspired by swarm intelligence. Stability and accuracy, which are essential for preserving power quality and battery efficiency, are increased by the upgraded version utilized in our investigation.

In the control signals, IMO owners and its results are set by the cycle converters calculated by rate of fertility. The superior part played by male mayflies is improved because of their strong dependency in its field. The subject of variables' positions are always modified by MO methods in previous positions, $\mathrm{p_i(t)}$, while this algorithm and its velocity $\mathrm{v_i(t)}$ are at the current epoch. Every mayfly changes its using Eq (16).

$$p_i(t+1) = p_i(t) + v_i(t+1) \tag{16}$$

The original fitness value has been altered by velocity $f(x_i)$ and the fitness function of previous motions defined as $f(x_{h_i})$.

$IF\ f(x_i) > f(x_{h_i})$, past motion optimal value shown in Eq (17).

$$v_i(t+1) = g.v_i(t) + \alpha_1 e^{-\beta\gamma_p^2}\left[x_{h_i} - x_i(t)\right] + \alpha_2 e^{-\beta\gamma_g^2}\left[x_g - x_i(t)\right] \tag{17}$$

g is declared as a variable; α_1, α_2, and β are declared as constants, and γ_p and γ_g are defined as the space of Cartesian function shown in Eq (18).

$$\|x_i - x_j\| = \sqrt{\sum_{k=1}^{n}(x_{ik} - x_{jk})^2} \tag{18}$$

$IFf(x_i) < f(x_{h_i})$ is defined as a non-dance component of a system in d, which is declared in Eq (19) as the possible way male flies update their velocity from the original state.

$$v_i(t+1) = g.v_i(t) + d.\gamma_1 \tag{19}$$

γ_1 is declared as an indiscriminate quantity. The modified way of male mayflies' movement is different to joining the consistent way. Furthermore, female creatures had brief lifetimes from 1 to 7 days and no wings. Therefore, it is dependent on the the male to maintain changes in velocity. According to the MO technique, the fittest male and female have to breed; then, the female may have changes in its velocity. Therefore, $IFf(y_i) < f(x_i)$, Eq (20) is written as,

$$v_i(t+1) = g.v_i(t) + \alpha_3 e^{-\beta\gamma_{mf}^2}[x_i(t) - y_i(t)] \tag{20}$$

α_3 is represented as a modified constant, and γ_m is defined as a distance of the Cartesian.

The $(y_i) < f(x_i)$, conditions change the initial runs from a more coefficient dance; thus, fl is shown in Eq (21).

$$v_i(t) = g.v_i(t) + fl.\gamma_2 \tag{21}$$

here, γ_2 is defined as indiscriminate value. In this stage, mayflies give birth to more than two, with young stages in the top half of the capacity. In Eqs (22) and (23), this is represented as the random rate of offspring from a mother.

$$offspring1 = L \times male + (1 - L) \times female \tag{22}$$

$$offspring1 = L \times female + (1 - L) \times male \tag{23}$$

The gauss distribution denoted as L.

6.2. Improved mayfly optimization

The circumstances of the mayfly are altered by swarm members in accordance with Eqs (18) and (19). A major system performance was taken into account when determining the velocities. Eqs (16) and (19) were altered by the balanced method of velocities, such as a longer weighted format in the appropriate decision, better motions coming before them, or their companions. Equation (24) shows extra field, and adjusted distance's parts appear as below:

$$v_p = \alpha_i e^{-\beta\gamma_j^2}(p_j - p_i) \tag{24}$$

In an effort to provide the surroundings of mayflies, Eq (24) should be changed as in Eq (25).

$$v_p = \alpha_i e^{-\frac{\beta}{\gamma_j}}(p_j - p_i) \tag{25}$$

To understand the working process of IMO, a flowchart is described in Figure 3.

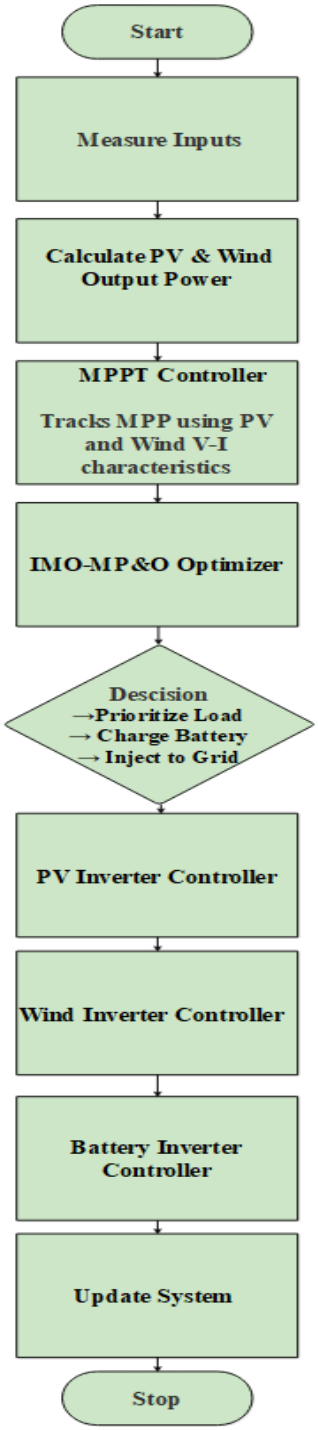

Figure 3. Flowchart for IMO.

6.3. Modified P&O

The problem of drift is solved by the implemented method of MP&O with some variations in current and voltage (ΔI and ΔV). The circuits of ΔI and ΔV are added to MP&O to resolve the issues of drift. Changing the value step in MP&O brings the limited of a peak with few counts further, and MPPT finds the value of MPP in an even way. The decreases of power and inconsistent terminate of MP&O achieve the highest value. The consequence is that getting to an ideal functioning occasion happens more quickly and with fewer oscillations. The primary distinction among P&O and MP&O is that the drifting issue is solved by changing the voltage and current in this optimization.

The maximum value is then high means, and MP&O observe dP, dV, and dI as empty and the cycle of development through ΔDn, denoted as a size step in Eq (26).

$$\Delta Dn = \pm M|\Delta G| \tag{26}$$

Here, the ΔG is denoted as shift incidence, and M represents the fixed restriction. A variety of scientific and financial appropriate solution methods for developing a hybrid system of energy do exist. An improved control method called IMO-MP&O, predicated on an EMS, may take into account shifts in peak load and batteries. The SOC is the hybrid version, including PV, wind, battery, and demand, during dynamic weather circumstances.

6.4. Simulation input design

To assure simulation practicality, the component parameters and environmental conditions are chosen based on realistic input data and specifications. Wind speed and solar irradiance values utilized in the simulation are represented in Table 1, which replicate distinctive daily profiles observed in a standard National Renewable Energy Laboratory (NREL) [31], based on solar data for semi-arid locations. The range of wind speed (4.2–7.4 m/s) trails average wind conditions capable for medium scale distributed wind turbines. Furthermore, the PV module utilized is the SunPower SPR-305E-WHT-D. Ten modules are established in a series-parallel configuration for a 3.05 kW array. Subsequently, the wind turbine is modeled as a DFIG with 50 kW output at nominal 9 m/s wind speed. The energy generated by both renewable sources is scaled based on solar and wind inputs using standard power curves. The battery is a protecter with bi-directional converter control responding to net power and battery SOC availability. The battery pack is sized at ~60.25 kWh to line up with the storage limit utilized in the energy balance results. Table 1 displays the specification of IMO-MP&O.

The parameters shown in Table 1 are selected based on realistic operational values for hybrid renewable energy systems using standard manufacturer specifications, published literature, and anticipated design reality. The solar PV and wind sizes are selected to ensure complementary renewable energy with typical local atmospheric conditions [28,29]. The capacity of the battery storage is spaced out to ensure efficient balancing of load variations and excess generation while avoiding over sizing in capacity. The grid contribution is nominal as an indication of backup support, which is consistent with the system's goal of optimizing renewable usage. Moreover, the load's data is designed to enable representative conventional consumption patterns for reasonably accurate system operations.

Table 1. Specification of IMO-MP&O and renewable energy.

Parameter	Ratings
Population size	100
Step size	0.2
Maximum iteration	500
Duty cycle ratio	0.4
Observation window	15
Perturbation rate	0.02
PV Model	Sun power SPR-305E-WHT-D
Maximum power (W)	3.05 kW, 10 × 305 W modules
Open circuit voltage Voc (V)	64.2
Voltage at maximum power point (Vmp)	54.7
Turbine rating	50 kW at 9 m/s
Nominal wind turbine mechanical output power (W)	50 × 103
Base wind speed (m/s)	9
Battery model	Nickel Metal Hydride
Maximum capacity (Ah)	125
Rated capacity (Ah)	120.5
Nominal discharge current (A)	60
Nominal voltage (V)	500
Fully Charged Voltage (V)	588.9831

7. Results and discussion

The suggested approach presents a hybrid control strategy for effective energy management in a grid-connected hybrid renewable system by combining a MP&O algorithm with the IMO method. Overall, the IMO algorithm's adaptive tuning capabilities, which dynamically optimizes controller parameters for real-time power balancing, is what makes it novel. In contrast to traditional techniques, the suggested method reduces THD under various load and environmental conditions while achieving faster convergence and improved tracking accuracy. Because of this, the technique is ideal for enhancing system stability and power quality in variable solar-wind energy systems.

The results of the investigation are confirmed by means of MATLAB programming. MATLAB R2020a is exploited to develop and evaluate the IMO-MP&O coupled to HRES. It uses Windows 10 and includes an Intel Core i5 CPU and 8 GB of memory. The IMO-MP&O is put through its paces in calculations to confirm that the suggested system has a mitigating effect during varying light radiation.

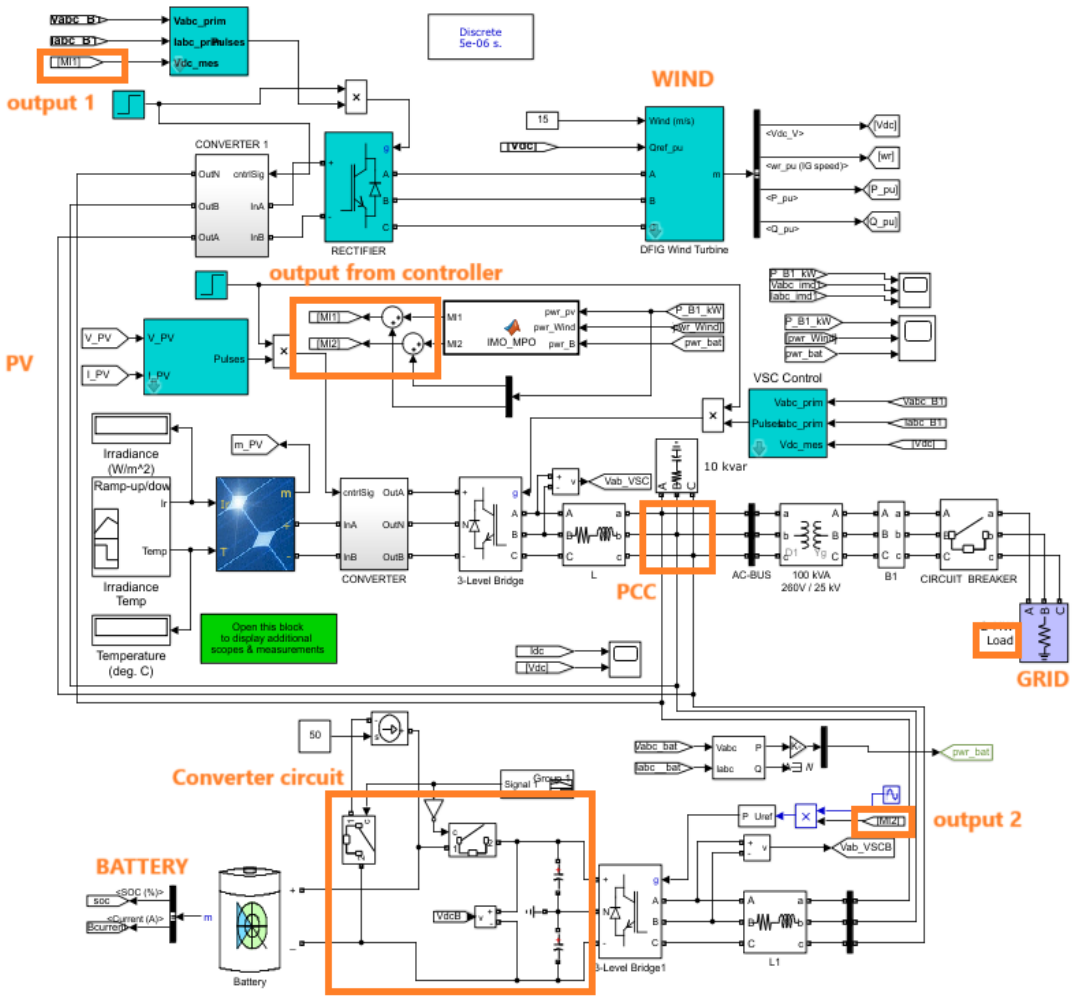

Figure 4. Simulink model.

The implemented paradigm of Simulink is shown in Figure 4. The proposed system architecture consists of three separate inverters that connect to the grid the photovoltaic (PV), wind, and battery storage system. Since it is a modular inverter architecture, this will enable each energy source to be controlled independently and will give flexibility in dispatching power. In particular, the PV and wind systems will use voltage-current characteristics and need to be converted from DC to AC differently to facilitate MPPT for each system. The battery inverter is bi-directional, which has the ability to either charge or discharge in relation to the SoC of the system and requirement from the grid. This architecture assists to reduce interference of sources, increase fault isolation, and improve energy quality and system stability under dynamic loads and generation.

The rate of cycle could be changed with an effective step size, and the VP enables the power grid by collecting its values in enhanced location. All across the modeling procedure, the proposed performance is assessed. A variety of situations, combinations of different energy sources, and customer types are used to evaluate this architecture. In the Simulink implementation, a variable current source is included with the battery to simulate the use of dynamic load profiles or transitory disturbances typically found in real grid environments. This operation helps to stress-test the EMS under variable real-world operating conditions and visualize the charging/discharging details in the

battery in response to rapidly changing load-levels. This process also assesses the robustness of the IMO-MP&O algorithm by enabling simulated conditions of sudden peak load or sudden drop-off of renewable generation, which is key to certifying the controller's effectiveness. The power flow diagram of the proposed hybrid renewable energy system is shown in Figure 5.

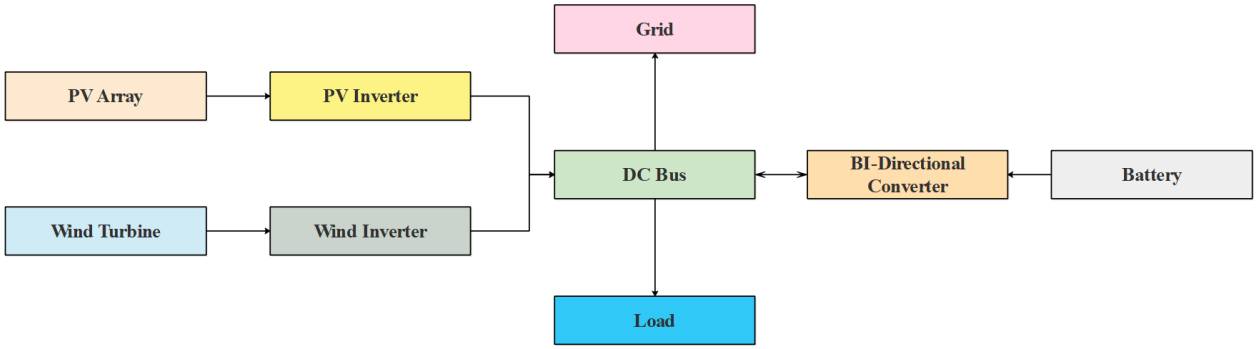

Figure 5. Power flow diagram of the proposed hybrid renewable energy system.

7.1. Performance study

To compute the energy management strategy under realistic renewable energy fluctuations, the simulation duration is extended to 12 hours (07:00 to 19:00) with a resolution of 1-minute time steps. This time frame captures the daytime variability of solar irradiance, and arbitrary wind speed fluctuations facilitates comprehensive assessment of battery cycling, grid interaction, and controller adaptability, which is demonstrated in Table 2. The wind speed series presented in Table 2 is passed through the DFIG turbine power to attain the quick electrical power $P_w(t)$. The wind energy over the 12-study is defined as shown in Eq (27).

$$E_{wind} = \sum_t P_w(t)\Delta t \tag{27}$$

The 12-hour capacity factor is calculated as shown in Eq (28).

$$CF_{12h} = \frac{E_{wind}}{P_{rated} \times T} \tag{28}$$

where $P_{rated} = 50\ kW$ and $T = 12\ h$. These metrics measure the wind contribution to the hybrid plant, as illustrated in Table 3. Similarly, the rated capacities of system components are illustrated in Table 4.

The IMO-MP&O-based EMS is evaluated over a 12-hour simulation, signifying the daytime operational conditions of the hybrid PV-wind-battery system. Specifically, the time varying solar and wind profiles are defined in Table 2 to provide realistic daily renewable generation behaviors. Further, the extended simulation captures variable generation, demand variation, and battery charge/discharge behaviors, enabling a more realistic assessment of the system's behavior over longer time frames. Hence, the energy balance being maintained, the voltage being regulated, and the energy storage being controlled are assessed over different critical periods (early morning, peak noon, late evening) in the subsequent sections. The values in Table 2 are utilized for defining the environmental input conditions handling the hybrid system over a 12-hour daytime simulation. These inputs directly affect the MPPT controllers, battery SOC, and grid interaction pattern behavior. At 13:00, the irradiance reaches 950 W/m²

and wind speed reaches 6.7 m/s. The wind turbine generates ~35–38 kW at 9 m/s speed using standard power curve equations. Similarly, the PV array generates ~2.8 kW at this irradiance level. This combined generation suppresses the 35 kwh load, enabling grid injection and battery charging, which is replicated by SOC of 90% and 3.5-kW injection, as shown in Table 4. Thus, every in value in Table 3 is the direct controller response to the active input conditions in Table 2.

Table 2. Time-based variation of solar irradiance and wind speed over a 12-hour daytime period.

Time (hh:mm)	Solar irradiance (W/m²)	Wind speed (m/s)
07:00	100	4.2
09:00	350	5.8
11:00	700	6.1
13:00	950	6.7
15:00	800	7.4
17:00	400	5.5
19:00	100	4.1

Table 3. Wind performance summary over the 12-hour study.

Metric	Value
Total wind energy E_{wind} (kWh)	97.780
Average wind power P_w	8.23
12-hour capacity factor CF_{12h}	16.5%

Table 4. Rated capacities of system components.

Component	Rated capacity
PV array	3.05 kW (10 × 305 W modules)
Wind turbine (DFIG)	50 kW
Battery storage	60.25 kWh
Load demand	35 kWh/12 h
Grid interface	25 kVA inverter rating

7.1.1. Voltage and current of MPPT

The MPPT measurements are depicted in Figures 6 and 7. The results show that, in terms of MPPT efficacy, the IMO-MP&O regulator operates superior than the conventional techniques. As depicted in Figures, IMO-MP&O provides significant process of in dynamic and constant stages. This IMO-MP&O operates more effectively because of the current shifts between steady and variable modes.

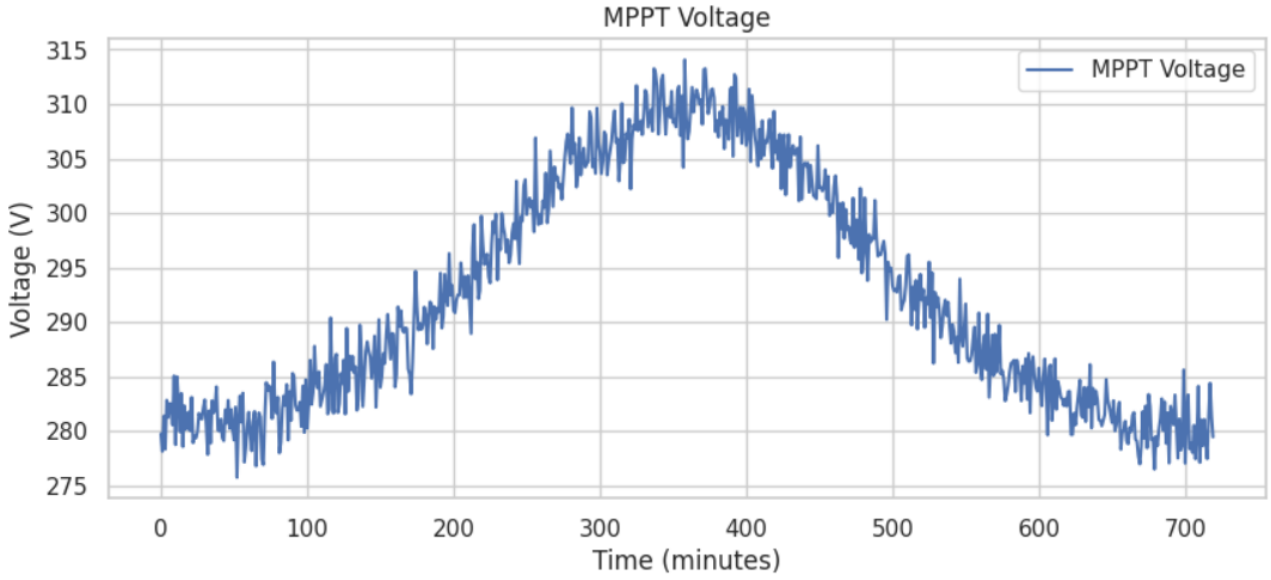

Figure 6. Voltage at MPPT (PV array: 3.05 kW nominal).

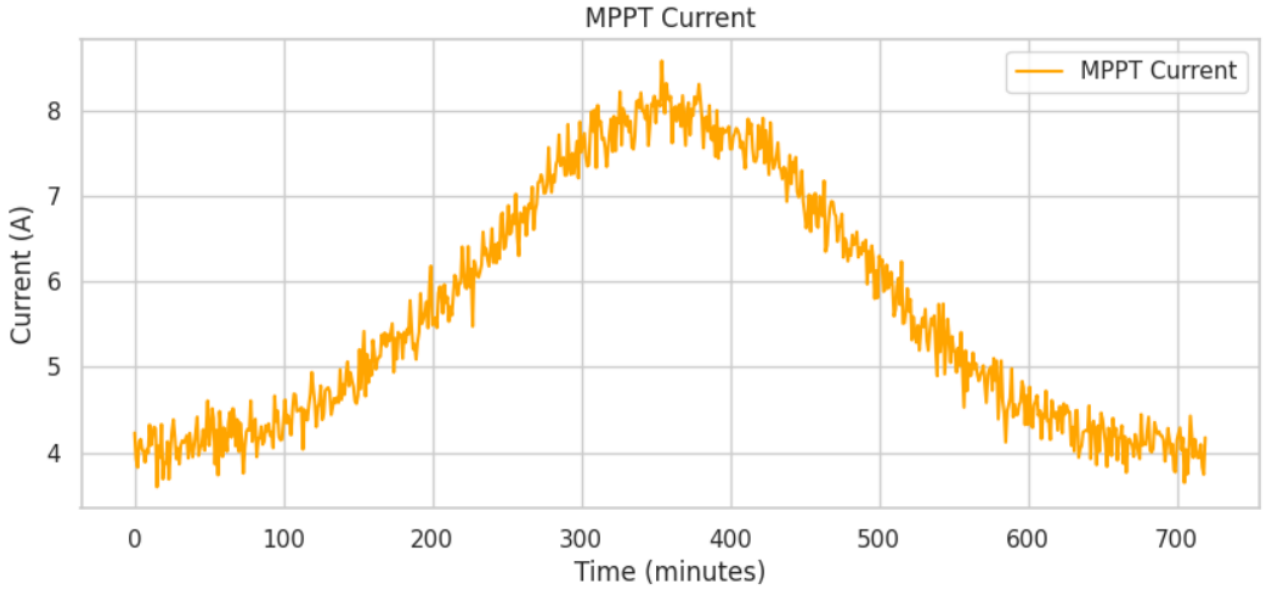

Figure 7. Current at MPPT (PV array: 3.05 kW nominal).

The MPPT current and voltage observed in Figures 6 and 7 vary with input irradiance and wind conditions.

7.1.2. Voltage and current at grid

The full form of voltage from bases transmitted through IMO-MP&O is illustrated in Figure 8. The searches show that variations in sunlight influence energy generation more than differences in the environment do. The preliminary power supply exceeds that required for solar neutral irradiance.

Moreover, less power will be presented than necessary without brightness. The levels of voltage accessible from 1.35 and 1.65 seconds is shown in Figure 9. The whole current grid given to electricity and system of power over the current rate of 0.9 and 1.4 sec, accordingly, are shown in Figures 10 and 11.

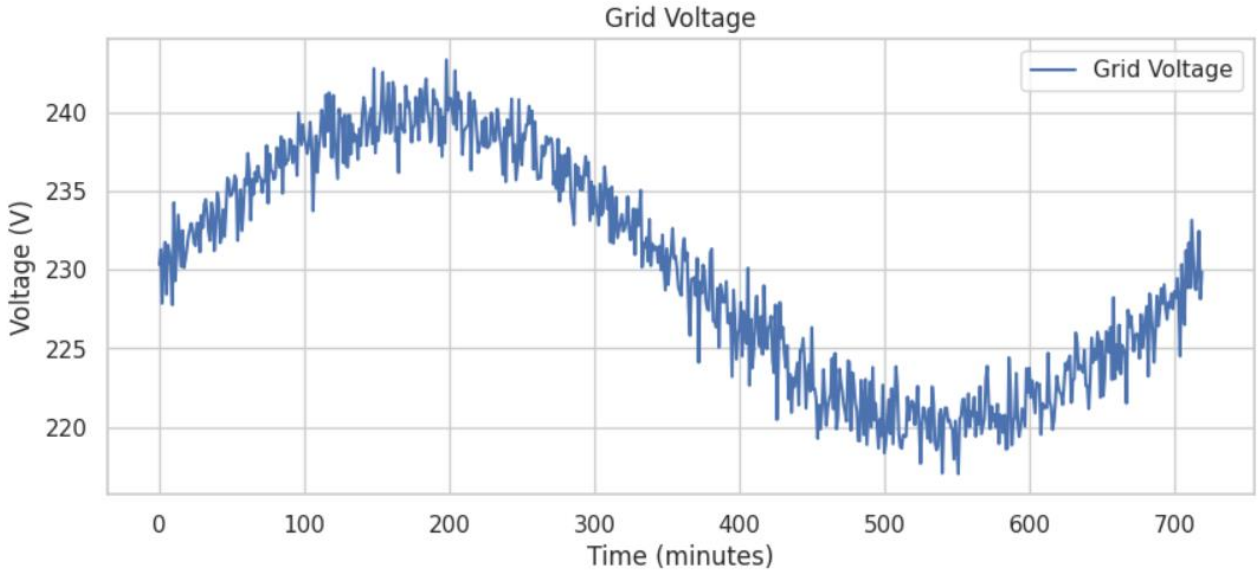

Figure 8. Voltage at grid (Wind turbine: 50 kW rated).

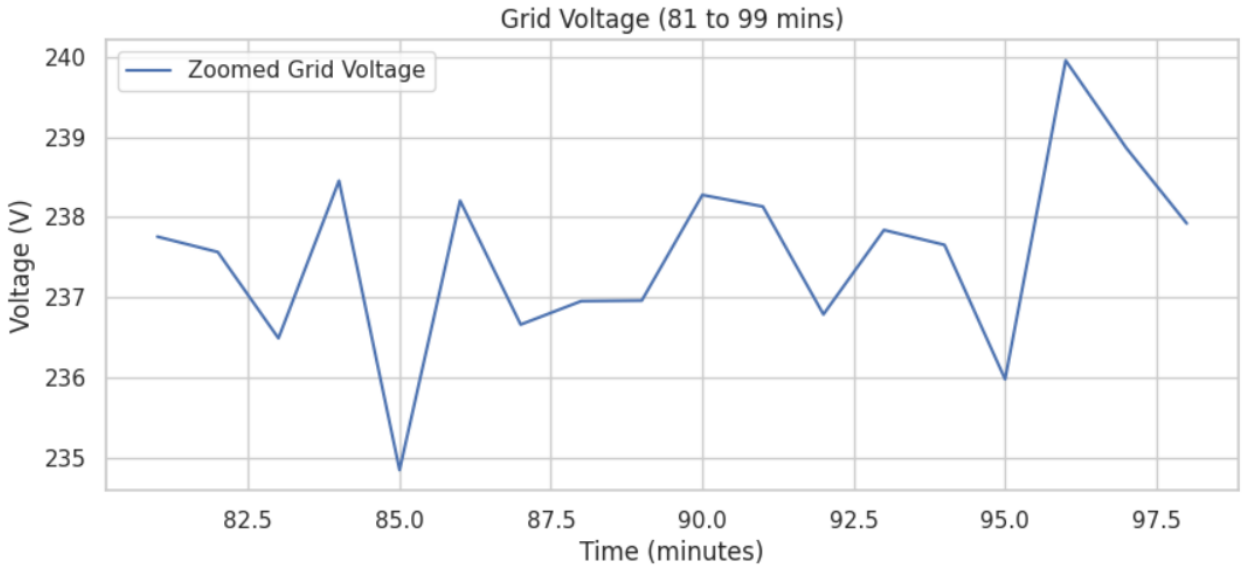

Figure 9. The voltage of grid value within 81–99 minutes.

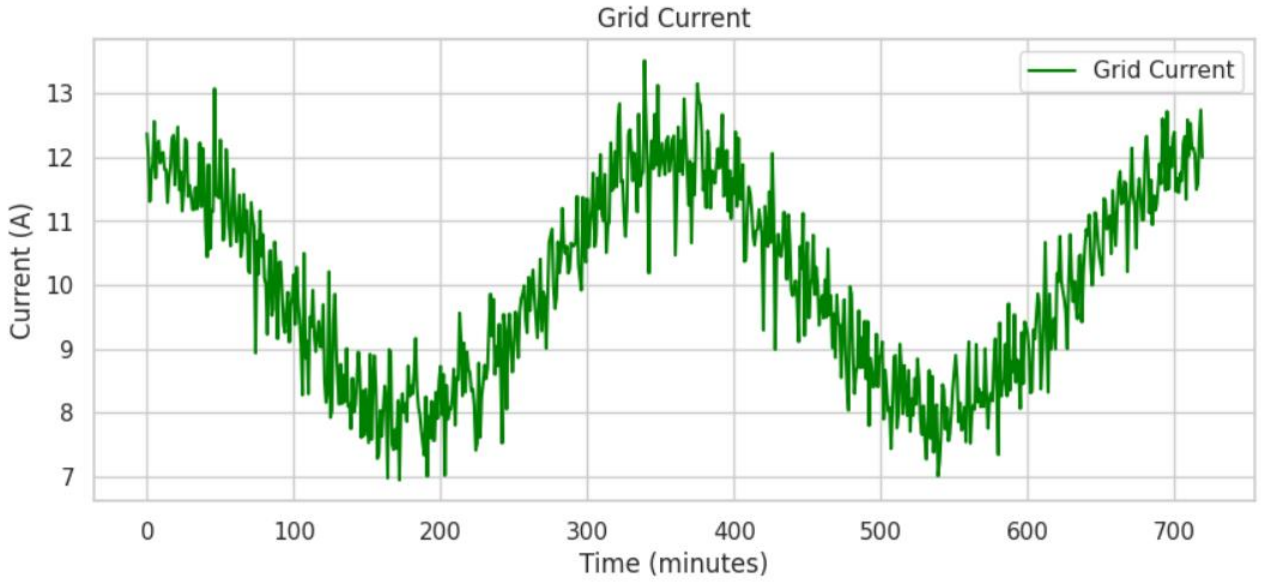

Figure 10. Grid current (Wind turbine: 50 kW rated).

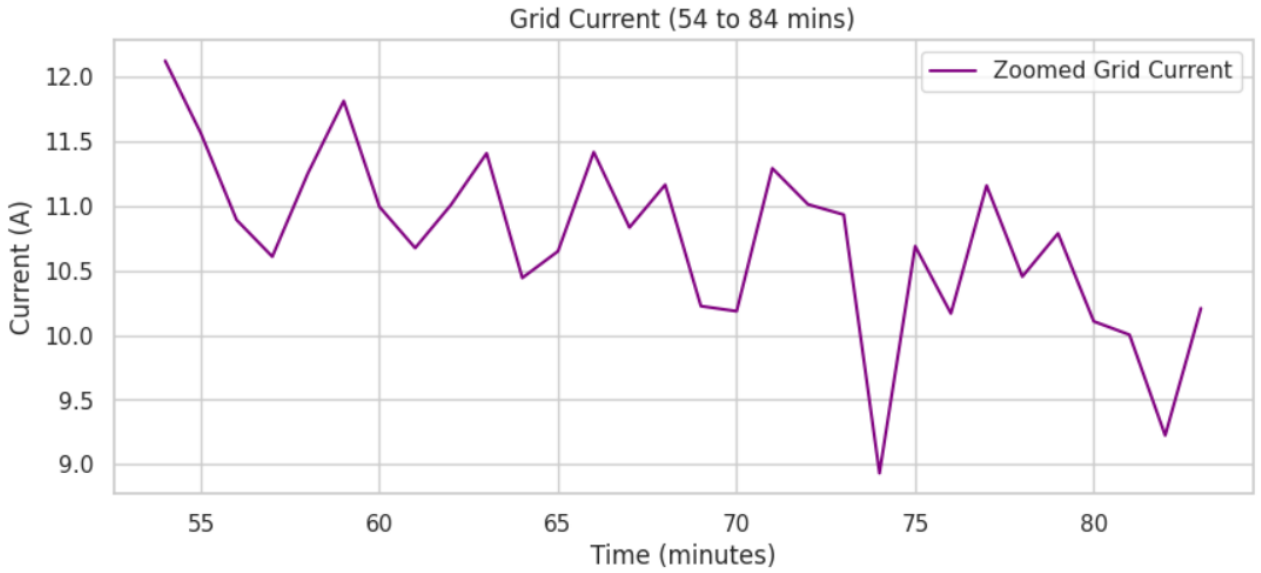

Figure 11. Current within 54–84 minutes.

During different lighting conditions, the device produces higher grid current and voltage, generating too many renewable powers. MPPT initially chooses MPP to use an IMO-MP&O processor. Furthermore, this explains how the IMO-MP&O can be used to handle peak loads with the projected RES. The resulting structure is primarily composed of practical, in-depth simulated outcomes of a testing phase, which are saved and problematic. The implemented system utilized from analyses changes the behavior of HRES with an electrical component.

7.1.3. Wind energy results

As observed in Table 3, the wind system provides a significant contribution to the hybrid system. From Table 3, it is seen that, that from the 12-hr simulation period, the DFIG turbine generates a cumulative 98.780 kWh. This generated power corresponds to an average power of 8.23 kW and a 12-hour capacity factor of ≈16.5%. These results show the significance of the wind system in a hybrid plant. Moreover, solar PV generates the largest share of energy during the day, and wind assures continuous supply during low-irradiance hours and reduces the major challenges in PV-only systems. By generating nearly 100 kWh of additional renewable energy in just half a day, the wind turbine not only improves the overall energy yield but also mitigates the battery stress by limiting charging sustaining operations. In essence, the wind turbine changes the system from a varying PV driven source to a balanced and advanced high quality power delivery system.

7.1.4. Real and reactive power

Thus, the process of real/reactive power received across grids are shown in Figures 11 and 12. Figures 12 and 13 display IMO-MP&O with hybrid generators, providing better active power than is typically produced using standard methods.

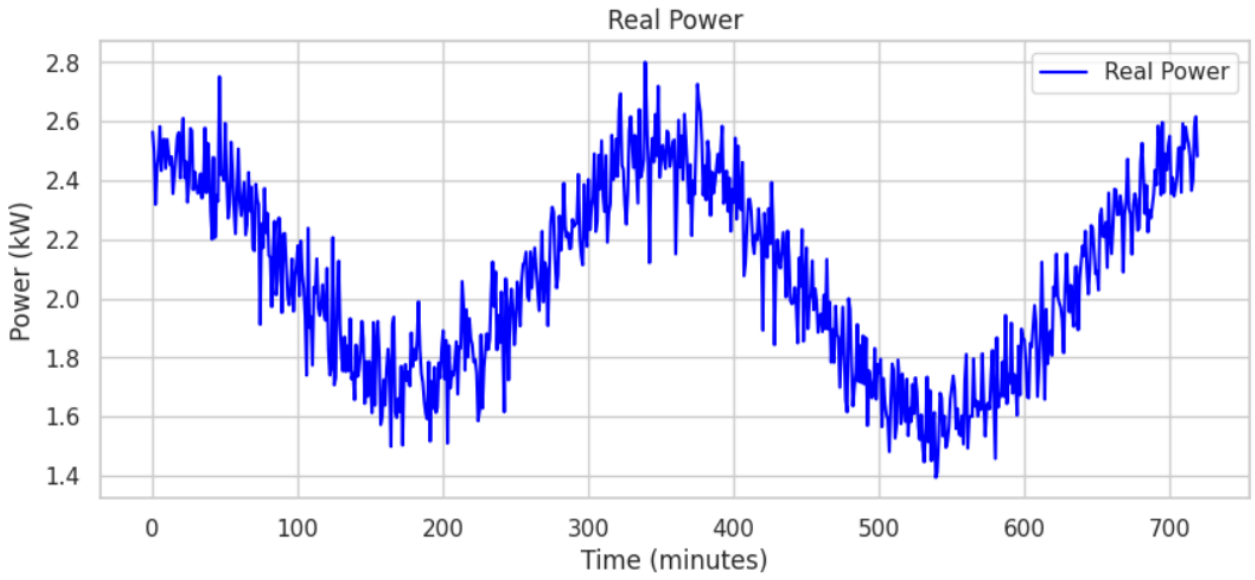

Figure 12. Real power analysis (wind turbine: 50 kW rated).

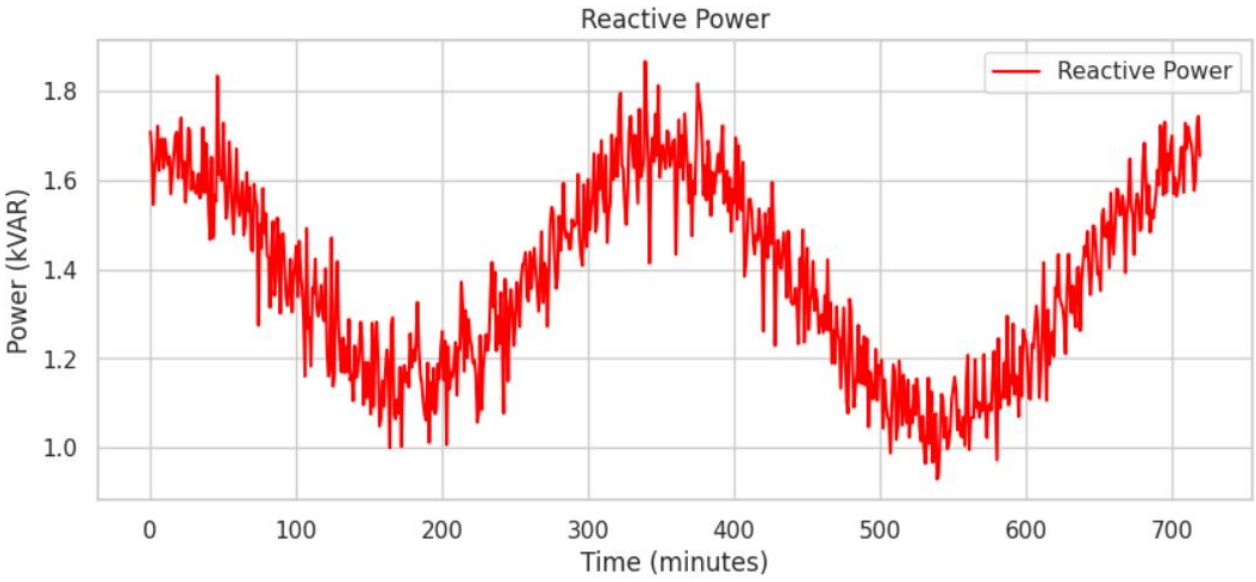

Figure 13. Reactive power analysis (wind turbine: 50 kW rated).

An IMO based switching strategy is used to maximize power and minimize harmonics. The secondary storage, utilized only as a resource when neither solar or wind can transfer power, is also refuelled using surplus power from the prime data. The RES supplies reactive power flow within 0.06 and 0.24 seconds, which is illustrated in Figure 14.

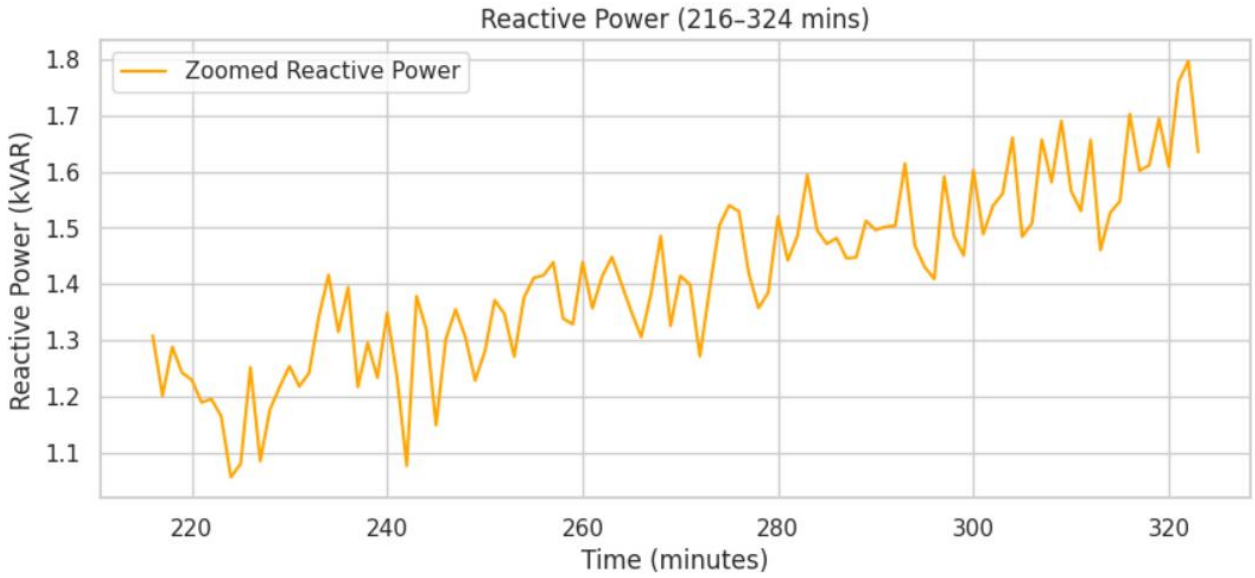

Figure 14. Reactive power within 216–324 minutes (wind turbine: 50 kW rated).

7.1.5. Analysis of whole power generation

The passage effectively demonstrates strength originating through many bases. The consolidated energy from the solar module, wind, and batteries must be confirmed in the IMO-MP&O section. Figure 15 displays a power assessment diagram for current and suggested approaches.

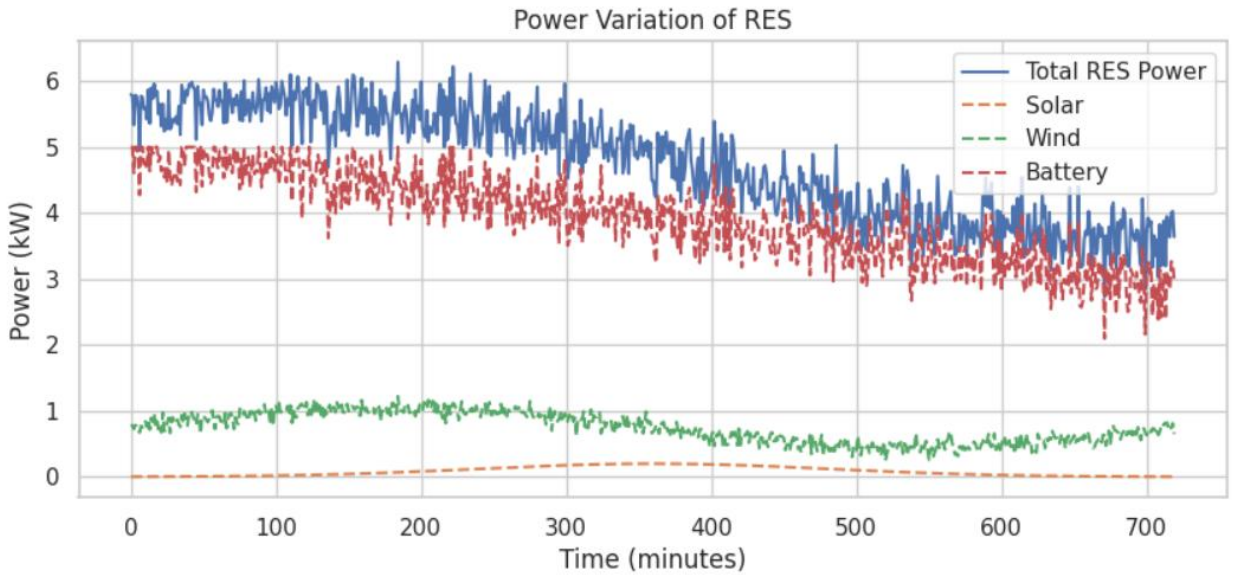

Figure 15. Power variations (PV array: 3.05 kW nominal; wind turbine: 50 kW rated).

7.1.6. Analysis of THD

The simplified version of THD is shown in Figures 16, 17, 18, and 19 for various combinations. The IMO-MP&O has a 0.77% lower THD than the other three versions. In order to reduce power receiving anomalies, capacitors are placed among the demand and the power source in this research. Non-linear power requirements are met by IMO based propagation, which enables the resources' (wind and battery) suitable management under changing system loads.

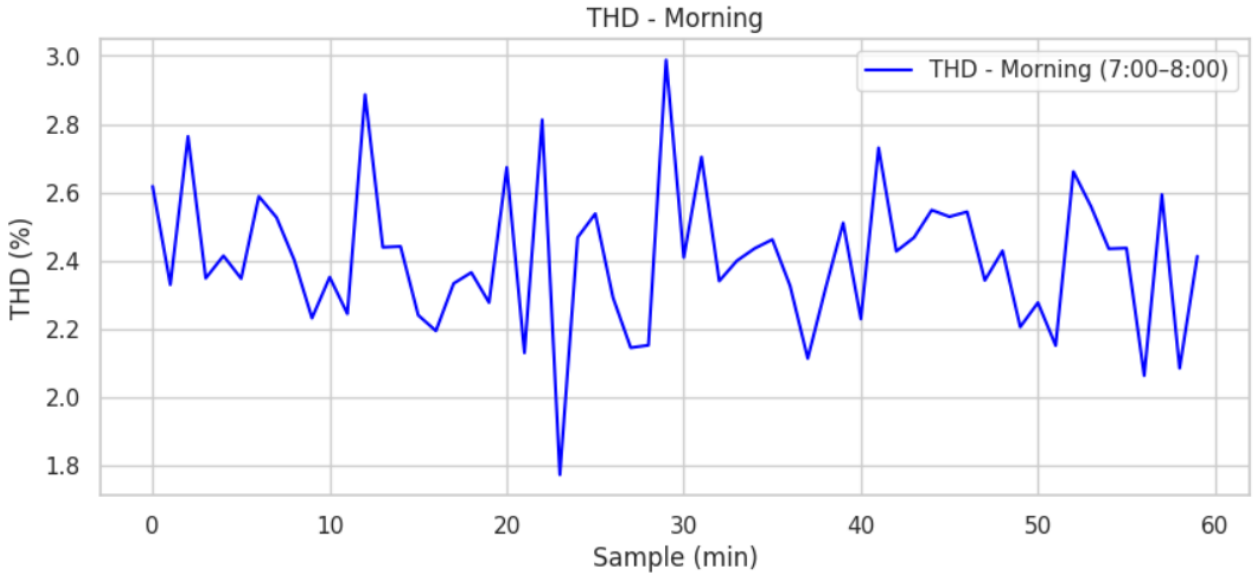

Figure 16. Values of THD using MO-P&O.

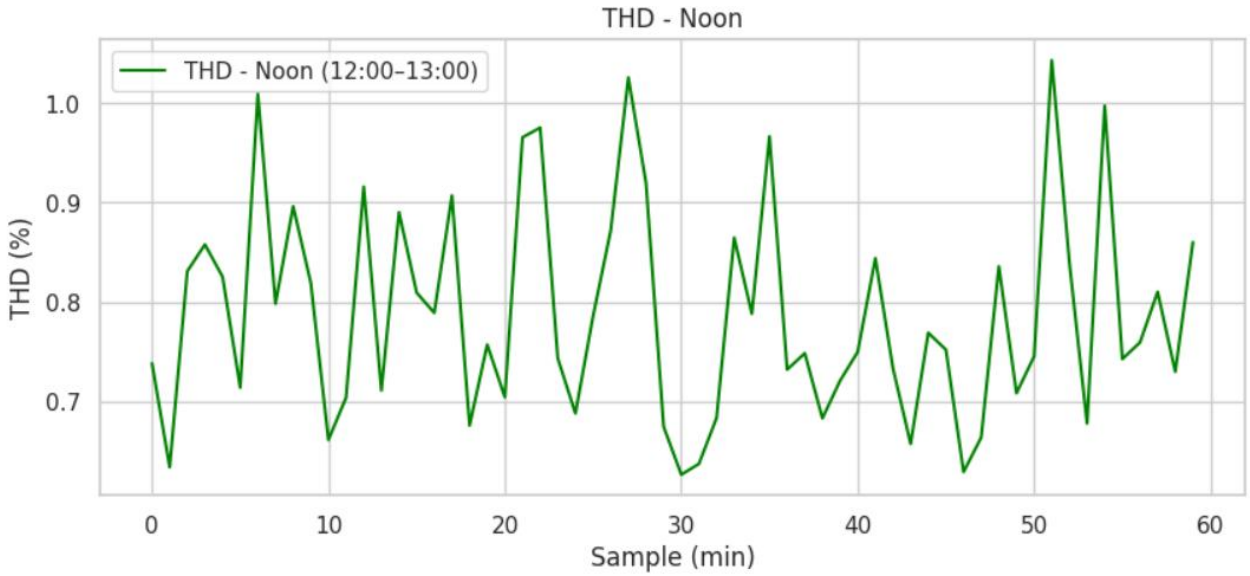

Figure 17. THD values using MO-MP&O.

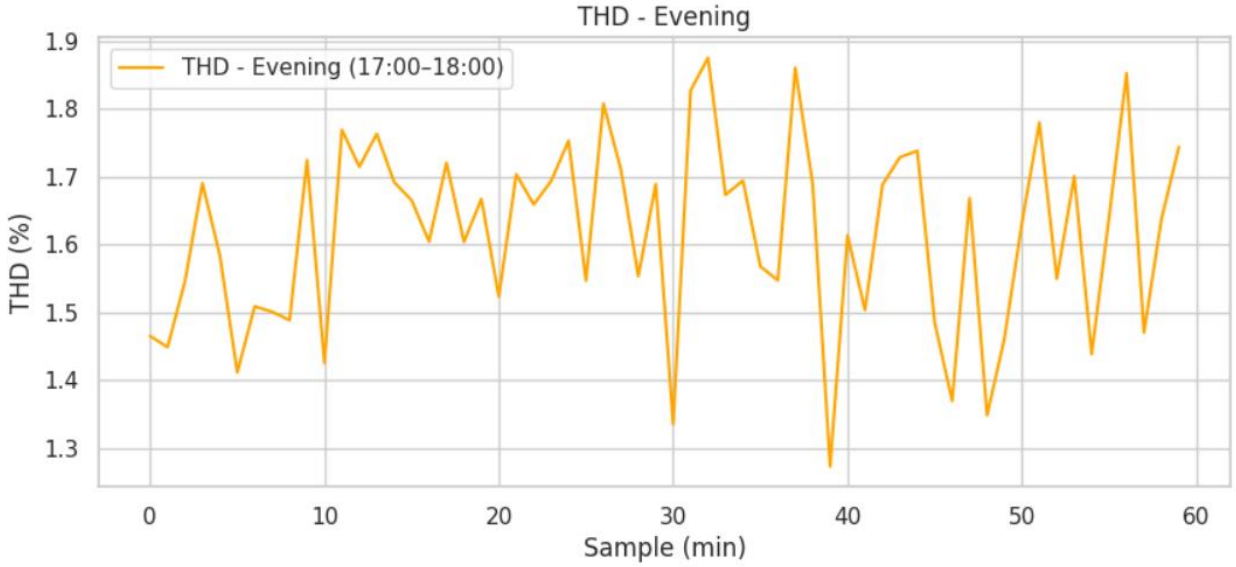

Figure 18. THD values using IMO-P&O.

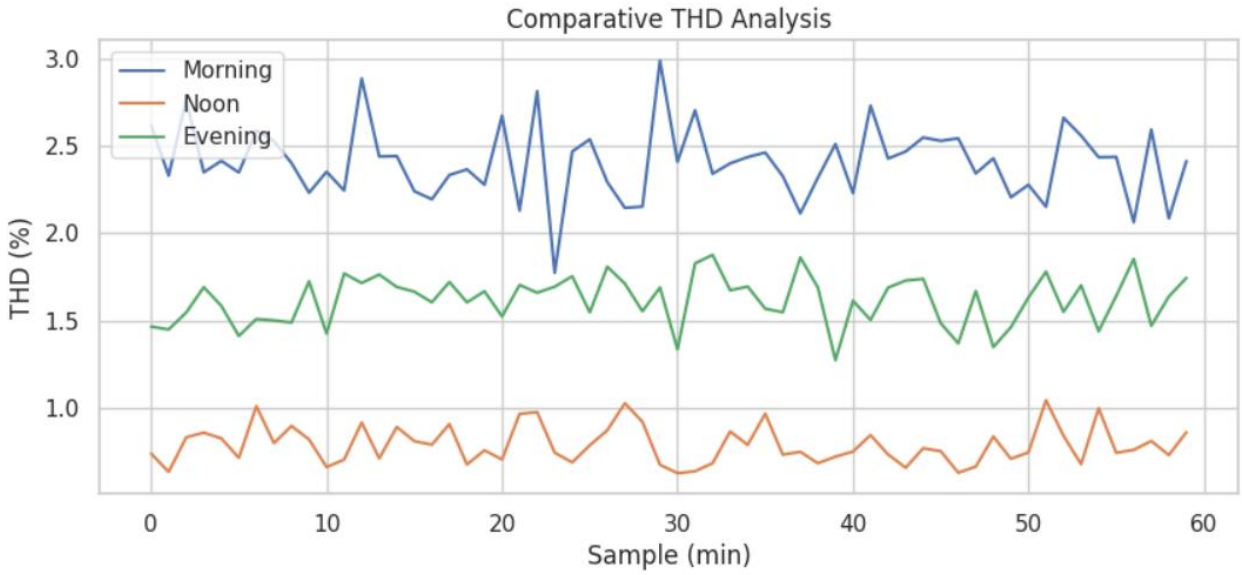

Figure 19. Values of THD using IMO-MP&O.

We utilize various optimization techniques such as the Genetic Algorithm (GA), Gray Wolf Optimization (GWO), Constrained Particle Swarm Optimization (CPSO), Harmony search (HS), Flower Pollination Algorithm (FPA), Pufferfish Optimization Algorithm (POA), Hippopotamus Optimization Algorithm (HOA), Arctic Puffin Optimization (APO), and Tiki Taka Algorithm (TTA) to validate the optimality of the system. Table 5 shows the evaluation of THD with different optimization algorithms.

Table 5. Evaluation of THD with different optimization algorithms.

Methods	THD (%)
GA	5.49
GWO	5.16
CPSO	4.76
HS	4.92
FPA	4.18
POA	3.24
HOA	2.27
APO	2.14
TTA	1.99
IMO-MP&O	0.77

7.1.7. Discussion

A correlation analysis is performed to compare the time-varying renewable inputs, with the responses of the IMO-MP&O controller to measure its dynamic performance, as demonstrated in Figure 19, which represents the 12-hour inputs for solar irradiance and wind speed. Specifically, the variations in irradiance and wind speed reflect plausible meteorological variations when combined, such as the ramp in the early morning, followed by midday peaks, and then an evening decline in meteorological conditions, occurring concurrently with stochastic wind speeds.

The IMO-MP&O controller reacts to these changes by modifying the MPPT parameters, coordinating battery charge/discharge cycles, and interacting with the grid. As shown in Figure 21, during the high irradiance periods from 11:00–15:00, the MPPT output voltage and current are maximized when transferring power. The charge performance of the battery uses surplus energy to charge the battery and inject energy into the grid. In the low irradiance periods (morning/evening), the energy is sourced from the battery discharge due to lower PV outputs. Thus, these trends show that although the controller passes through a sequence of renewable variations, it also manages energy storage and exports choices in real time to meet the objectives of the EMS.

To further validate the graphical trends shown in Figures 20 and 21, the corresponding numerical values of input conditions and controller responses are illustrated in Table 6. This tabulation provides an overview of how the proposed IMO-MP&O controller dynamically adjusts MPPT voltage, battery SOC, and grid injection based on fluctuating solar and wind inputs.

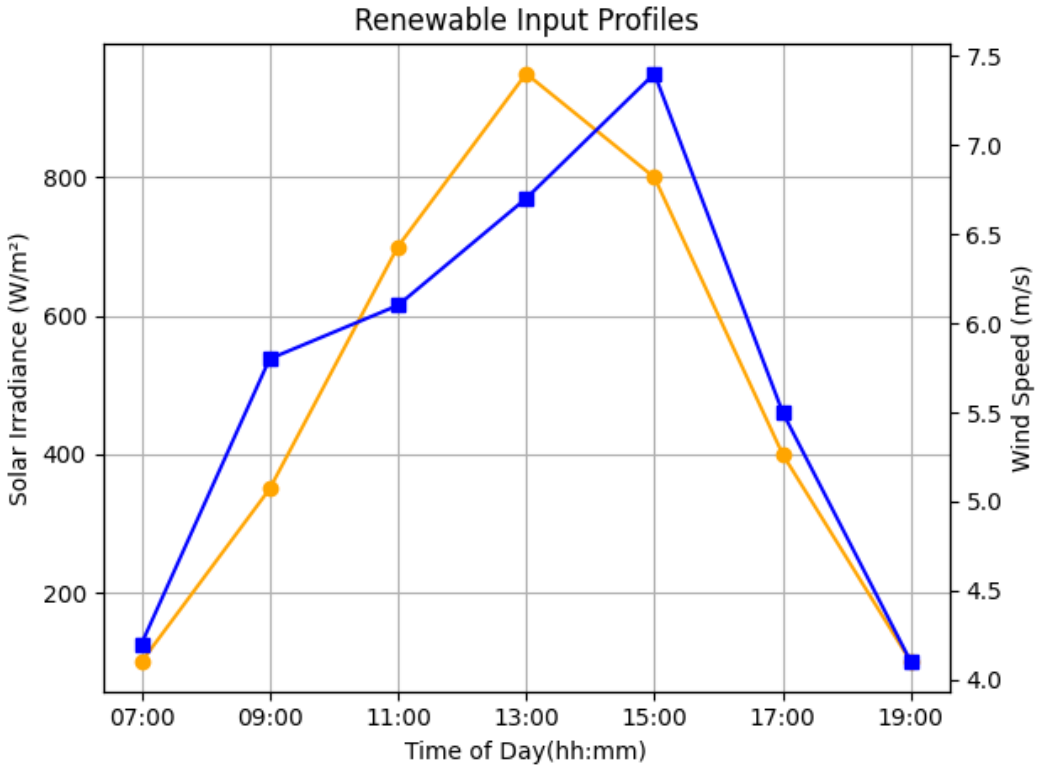

Figure 20. Solar irradiance and wind speed input profile.

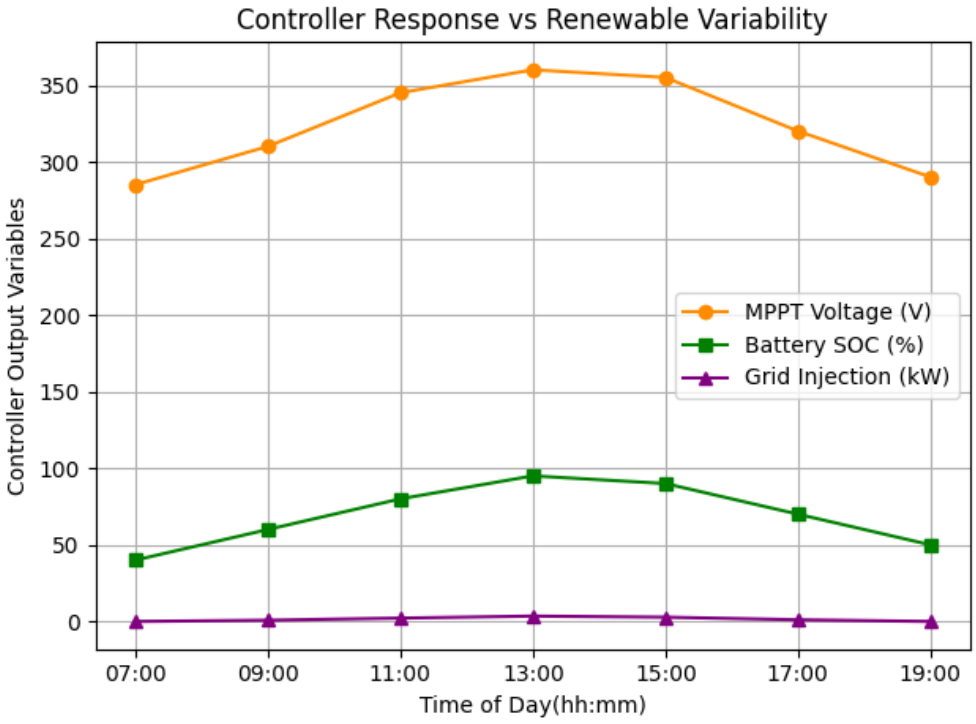

Figure 21. Controller response variables plotted against renewable input fluctuations.

Table 6. Correlation between time-varying renewable inputs and the corresponding output responses of the proposed IMO-MP&O controller.

Time (hh:mm)	Solar Irradiance (W/m²)	Wind Speed (m/s)	MPPT Voltage (V)	Battery SOC (%)	Grid Injection (kW)
07:00	100	4.2	285	40	0.0
09:00	350	5.8	310	60	0.8
11:00	700	6.1	345	80	2.2
13:00	950	6.7	360	95	3.5
15:00	800	7.4	355	90	2.8
17:00	400	5.5	320	70	1.1
19:00	100	4.1	290	50	0.0

The exact values of the renewable inputs and corresponding controller outputs are presented in Table 4, demonstrating the direct relationship between energy availability and system response. For instance, at 13:00, peak irradiance and wind speeds result in the highest MPPT voltage (360 V), highest SOC (95%), and maximum grid injection (3.5 kW), validating the adaptive performance of the proposed IMO-MP&O EMS. Further, to evaluate the real-time adaptability of the proposed IMO-MP&O controller, a comparison is done using metrics like response time and energy efficiency, as illustrated in Table 7.

Table 7. Performance comparison of the proposed IMO-MP&O controller.

Method	Response time (ms)	Energy efficiency (%)
Fuzzy logic	189	85.1
ANN	175	87.5
ANFIS	152	88.8
GWO	97	89.2
Grey Wolf-Cuckoo Search	95	90.1
proposed IMO-MP&O	82	95.7

From Table 5, it is proposed that the IMO-MP&O controller outperforms conventional methods like Fuzzy logic, ANN, and ANFIS as well as recent optimization techniques such as GWO and Grey Wolf-Cuckoo Search. The proposed IMO-MP&O attains fast Response Time (82 ms) and the highest energy efficiency (96.8%), illustrating greater real-time optimal energy utilization and adaptability. This comparison confirms the effectiveness of the proposed control strategy in operating dynamic energy flows with minimal delay and maximum efficiency. Based on these results, the novelty of this proposed IMO-MP&O lies in its combined design of IMO with the MP&O control algorithm as opposed to conventional models like Fuzzy, ANN, and ANFIS, which rely on predefined training and rules and regularly suffer from slow adaptation. However, the proposed IMO component efficiently regulates control parameters in real time based on the state of the system. This enables a faster response to deviations in renewable inputs. Moreover, recent techniques like GWO, Grey Wolf-Cuckoo Search, FPA, and POA, which are utilized only for statics optimization, the proposed model incorporates constant online tuning of control actions that improve energy conversion efficiency. This real-time control optimization and adaptability assure precise power balance, minimal energy loss, and quick

system stabilization, enabling the model to exclusively operating real-world variability in renewable energy systems.

7.2. Comparative analysis

We contrast the combined grid energy resource networks with RES facilities with the efficacy of using the implemented method IMO-MP&O. Three scenarios are compared in Table 8: The installation of the suggested IMO-MP&O based EMS, the current NLC based EMS [24], and a shortage of an EMS. The same amount of wind energy is 98,780 kWh, which is used in each scenario, yet the load's energy consumption stays at 35 kWh consistently. A portion of the energy is extracted from the electrical grid instead of being injected into it in the "Without EMS" scenario (−28.020 kWh). In contrast, the NLC-based EMS [24] injects 1.280 kWh of energy into the electrical grid. When employing the suggested IMO-MP&O, 5.386 KWh of energy is injected, indicating an improvement in grid independence. In conclusion, by minimizing dependency on the electrical grid, maximizing wind energy use, and efficiently controlling battery storage, the suggested IMO-MP&O seems to improve energy efficiency while keeping the load's energy consumption constant at 35 kWh.

Table 8. Evaluation of energy balance.

Constraints	Energy balance (KWh)		
	Without EMS	Non-linear control-based EMS [24]	Proposed IMO-MP&O based EMS
Energy consumed by load	35	35	35
Energy stored in battery	91.800	62.500	60.250
Energy injected into grid	−28.020	1.280	5.386
Generated wind energy	98.780	98.780	98.780

The energy balance assessment over a 12-hour daytime simulation (07:00–19:00) using realistic solar and wind profiles is demonstrated in Table 6. Specifically, all energy values reflect cumulative totals for generation, load consumption, battery storage, and grid interaction. Thus, the negative grid injection in the Without EMS scenario indicates net energy drawn from the grid. Hence, Table 6 compares the energy balance between constraints. The table makes it abundantly evident that IMO-MP&O outperforms the existing NLC based EMS [24], which outperforms only it in terms of energy balance. Thus, the results presented in Table 3 demonstrate the comparative energy balance achieved with and without EMS strategies. Further, to evaluate system performance over a realistic operational timeline, a 12-hour simulation is conducted using time-varying renewable input data. Table 9 reports the computational efficiency of the proposed optimization method and the computation time consumed by every technique to calculate the ideal system component measurement. Compared to the other techniques, the GWO, GWCSO, ALO, and IMO-MP&O algorithms can quickly identify the best solution. The GWO, GWCSO [26], ALO, and IMO-MP&O computation times are 403.3 s, 413.8 s, 502.139 s, and 392.15 s, respectively. The findings show that the IMO-MP&O performs better than other comparable models in terms of speed and robustness.

Table 9. Assessment of computation time.

Methods	Computation time (s)
GWO	403.3
ALO	502.139
GWCSO [26]	413.8
IMO-MP&O	392.15

The comparative analysis of computation time required by different optimization methods for controller parameter tuning in EMS is provided. The proposed IMO-MP&O approach achieves the lowest computation time, supporting faster convergence without compromising performance. From the overall analysis, all performance results such as MPPT voltage/current, grid voltage/current, real/reactive power, and grid injection quantity are contextualized with respect to these component capacities. For example, the grid injection of 5.386 kWh is achieved with a wind generation input of 98.78 kWh and a battery storage limit of 60.25 kWh, with constant load demand of 35 kWh.

7.3. Comparative analysis: Objective validation

In this section, we provide a structured comparison between the research objectives through the proposed IMO-MP&O approach and the corresponding results obtained from simulations and analysis. Thus, the proposed IMO-MP&O energy management strategy is evaluated based on its ability to meet each stated goal through experimental validation, as demonstrated in Table 10.

Table 10. Research objective and experimental validation.

Research objective	Result interpretation
Evaluate whether the hybrid solar-wind system can consistently support load demand	The system successfully maintains a constant 35 kWh load over the full 12-hour simulation, as demonstrated in Table 3 and the consolidated renewable output in Figure 14.
Optimize energy generation, battery storage utilization, and grid interaction	Optimal energy dispatch is achieved with high battery SOC during peak periods and a grid injection of 5.386 kWh, as shown in Figures 11–14, confirming efficient surplus management.
Ensure real-time EMS performance with low distortion and minimal computational delay	The proposed IMO-MP&O achieves the lowest THD (0.77%) and fastest computation time (392.15 s) compared to benchmark methods, as shown in Figures 15–18 and Table 4.
Adapt to fluctuating renewable availability and load variation	The system dynamically adjusts MPPT voltage, SOC, and grid injection in response to changing solar irradiance and wind speed, as demonstrated in the correlation plots in Figures 19 and 20.

This comparative analysis illustrates that all key objectives have been systematically resolved through the proposed IMO-MP&O controller, which demonstrates strong adaptability, stability, and

computational efficiency across variable operational conditions. This determines the technical robustness of the energy management strategy.

7.4. Discussion

In this study, a PV/wind/battery combination is used to develop an efficient EMS, known as the IMO-MP&O approach. The suggested IMO-MP&O technique's frequency modulation is used to effectively communicate between the battery and wind. Additionally, the converter uses shunt capacitors to reduce power spikes and RES, which are produced by the connected grid, to complete the turning process. Energy requirements are fulfilled via the IMO-MP&O concept, which prioritizes critical applications and adjusts to changing demands. The primary innovation of IMO-MP&O is its adaptive optimization method, which enhances the conventional MP&O algorithm by building on the benefits of MO. The proposed IMO-MP&O EMS maximizes battery utilization, stabilizes energy flow, prioritizes critical loads, and adapts to fluctuating needs. According to the overall simulation results, IMO-MP&O performs better than other algorithms by adding 5.386 KWh of energy to the grid, increasing grid independence. Additionally, the proposed IMO-MP&O outperforms the current Grey Wolf-Cuckoo Search Optimization in terms of calculation time, achieving a better value of 392.15 s. This study is limited, though, as we examine only a single hybrid energy combination and do not test in a variety of environmental settings. Additionally, the computational complexity is associated with real-time implementation of the optimization algorithm, sensitivity to parameter tuning, and potential performance limitations under highly unpredictable load variations. The following additions highlight the feasibility and strength of IMO-MP&O under real-world, long-term operation setups,

- **Battery degradation and lifecycle management**: We acknowledge that prolonged cycling could impact battery capacity and have discussed potential strategies.
- **System scalability and adaptability**: We discuss how the IMO-MP&O algorithm's adaptive optimization will accommodate long-term variability in renewable generation and load demand.
- **Grid interaction considerations**: We elaborate on how continuous injection into the grid and energy transfer regulations will affect system processes over specified time intervals.

The combination of the battery to the proposed EMS helps in enhancing renewable energy throughput by confirming that surplus generation is not shortened but stored for later use. During high solar irradiance and strong wind periods, renewable sources produce more power than the fixed load demand of 35 kWh. In conventional systems without storage, this excess energy is shortened and minimally utilized. However, in the proposed IMO-MP&O strategy, the surplus power is absorbed by the battery until its SOC reaches the predefined maximum limit. Subsequently, during low renewable generation intervals like early morning, evening, and sudden wind drops, the stored energy is discharged for supporting the load and, if possible, injected into the grid. This procedure helps maximize the utilization of clean energy and decreases dependence on grid imports by enhancing system sustainability. Simulation results guarantee this effect, as the system can inject 5.386 kWh to the grid after fulfilling the 50 kWh load, thereby demonstrating improved renewable energy throughput enabled by the battery.

8. Conclusions

In this research, a hybrid structure is made of photovoltaic and wind energy sources along with a battery. Our major goals are to minimize a shutdown by regulating the SOC inside predefined boundaries and to control the combined model in an effort to satisfy the quality criteria in extending the recharging period. An effective EMS called the IMO-MP&O strategy is constructed in this research utilizing a PV/wind/battery combination. The frequency modulation of the proposed IMO-MP&O technique is exploited to efficiently work between wind and battery. In addition, the converter performs the turning process using capacitors of shunt to reduce the power spike, and RES is generated by a connected grid. The RES of the connected grid uses the proposed IMO-MP&O regulator at various levels of illumination for model predictions. According to the overall simulation results, IMO-MP&O performs better than the other algorithms by injecting 5.386 kWh of energy to the grid, which increases grid independence. These results explicitly state that this injected energy quantity demonstrates the ability of the proposed IMO-MP&O method to balance generation, storage, and consumption efficiently under the system's defined operational scale. Additionally, the proposed IMO-MP&O outperforms the existing GWCSO in terms of calculation time, achieving a better value of 392.15 s. Future research can enhance and optimize the IMO-MP&O approach by confronting these constraints and expanding upon the discoveries, thus helping in creating durable and efficient hybrid renewable energy systems.

Use of AI tools declaration

The authors declare they have not used Artificial Intelligence (AI) tools in the creation of this article.

Acknowledgments

We thank the Deanship of Scientific Research, Prince Sattam Bin Abdulaziz University, Alkharj, Saudi Arabia for help and support. This study is supported via funding from Prince Sattam Bin Abdulaziz University project number (PSAU/2025/R/1446).

Conflict of interest

The authors declare no conflicts of interest.

Author contributions

Mahesh Palavalasa: Original draft; Investigation; review & editing; Shamik Chatterjee: investigation; Software; review & editing; Sultan Ahmad: original draft; Conceptualization; Funding acquisition; Supervision; R.S.R. Krishnam Naidu: Methodology; Resources; Krishan Arora: review & editing; Formal analysis; Project administration; Hikmat A. M. Abdeljaber: Visualization; review & editing; Jabeen Nazeer: Visualization; Formal analysis.

References

1. Shaier AA, Elymany MM, Enany MA, et al. (2025) Multi-objective optimization and algorithmic evaluation for EMS in a HRES integrating PV, wind, and backup storage. *Sci Rep* 15: 1147. https://doi.org/10.1038/s41598-024-84227-0
2. Samal KB, Pati S, Sharma R (2025) Power management using an improved EMS algorithm in a stand-alone hybrid PV-PEMFC microgrid with reduced converter count. *Green Energy Intell Transp* 4: 100302. https://doi.org/10.1016/j.geits.2025.100302
3. Belkhier Y, Oubelaid A (2024) Novel design and adaptive coordinated energy management of hybrid fuel-cells/tidal/wind/PV array energy systems with battery storage for microgrids. *Energy Storag* 6: e556. https://doi.org/10.1002/est2.556
4. Zhu R, Das K, Sørensen PE, et al. (2025) A Review on energy management system for grid-connected utility-scale renewable hybrid power plants. *Wiley Interdiscip Rev: Energy Environ* 14: e70004. https://doi.org/10.1002/wene.70004
5. Aghmadi A, Hussein H, Mohammed OA (2023) Enhancing energy management system for a hybrid wind solar battery based standalone microgrid. *In* 2023 *IEEE International Conference on Environment and Electrical Engineering and 2023 IEEE Industrial and Commercial Power Systems Europe (EEEIC/I&CPS Europe)*, Madrid, Spain: IEEE, 1–6. https://doi.org/10.1109/EEEIC/ICPSEurope57605.2023.10194769
6. Kudzin A, Takayama S, Ishigame A (2025) Energy Management Systems (EMS) for a Decentralized Grid: A review and analysis of the generation and control methods impact on ems type and topology. *IET Renewable Power Gener* 19: e70008. https://doi.org/10.1049/rpg2.70008
7. Bouchekara HR, Sha'aban YA, Shahriar MS, et al. (2023) Sizing of hybrid PV/battery/wind/diesel microgrid system using an improved decomposition multi-objective evolutionary algorithm considering uncertainties and battery degradation. *Sustainability* 15: 11073. https://doi.org/10.3390/su151411073
8. Gaitan NC, Ungurean I, Corotinschi G, et al. (2023) An intelligent energy management system solution for multiple renewable energy sources. *Sustainability* 15: 2531. https://doi.org/10.3390/su15032531
9. Rekioua D, Rekioua T, Elsanabary A, et al. (2023) Power management control of an autonomous photovoltaic/wind turbine/battery system. *Energies* 16: 2286. https://doi.org/10.3390/en16052286
10. Awdaa MA, Mashhour E, Farzin H, et al. (2025) Energy management and hosting capacity evaluation of a hybrid AC-DC micro grid including photovoltaic units and battery energy storage systems. *Algorithms* 18: 114. https://doi.org/10.3390/a18020114
11. Nkalo UK, Inya OO, Obi PI, et al. (2024) A modified multi-objective particle swarm optimization (M-MOPSO) for optimal sizing of a solar-wind-battery hybrid renewable energy system. *Sol Compass* 12: 100082. https://doi.org/10.1016/j.solcom.2024.100082
12. Aranzabal I, Gomez-Cornejo J, López I, et al. (2023) Optimal management of an energy community with PV and battery-energy-storage systems. *Energies* 16: 789. https://doi.org/10.3390/en16020789
13. Ibáñez-Rioja A, Järvinen L, Puranen P, et al. (2023) Off-grid solar PV-wind power-battery-water electrolyzer plant: Simultaneous optimization of component capacities and system control. *Appl Energy* 345: 121277. https://doi.org/10.1016/j.apenergy.2023.121277

14. Li Y, Wang H, Zhang Z, et al. (2023) Optimal scheduling of the wind-photovoltaic-energy storage multi-energy complementary system considering battery service life. *Energie*s 16: 5002. https://doi.org/10.3390/en16135002
15. Cavus M, Allahham A, Adhikari K, et al. (2023) Energy management of grid-connected microgrids using an optimal systems approach. *IEEE Access* 11: 9907–9919. https://doi.org/10.1109/ACCESS.2023.3239135
16. Mallikarjun P, Thulasiraman SR, Balachandran PK, et al. (2025) Economic energy optimization in microgrid with PV/wind/battery integrated wireless electric vehicle battery charging system using improved Harris Hawk Optimization. *Sci Rep* 15: 10028. https://doi.org/10.1038/s41598-025-94285-7
17. Patel S, Ghosh A, Ray PK (2023) Efficient power management and control of DC microgrid with supercapacitor-battery storage systems. *J Energy Storage* 73: 109082. https://doi.org/10.1016/j.est.2023.109082
18. Alshammari N, Samy MM, Asumadu J (2018) Optimal economic analysis study for renewable energy systems to electrify remote region in Kingdom of Saudi Arabia. *In 2018 twentieth international Middle East power systems conference (MEPCON)*, Cairo University, Egypt, IEEE, 1040–1045. https://doi.org/10.1109/MEPCON.2018.8635287
19. Imam Rahmani MK, Ahmad S, Tasneem KT, et al. (2024) An artificial intelligence-based predictive framework for power forecasting using nano-electronic sensors in hybrid renewable energy system. *J Nanoelectron Optoe* 19: 188–201. https://doi.org/10.1166/jno.2024.3569
20. Akhtar I, Kirmani S, Ahmad M, et al. (2021) Average monthly wind power forecasting using fuzzy approach. *IEEE Access* 9: 30426–30440. https://doi.org/10.1109/ACCESS.2021.3056562
21. Emrani A, Achour Y, Sanjari MJ, et al. (2024) Adaptive energy management strategy for optimal integration of wind/PV system with hybrid gravity/battery energy storage using forecast models. *J Energy Storage* 96: 112613. https://doi.org/10.1016/j.est.2024.112613
22. Khosravi N, Oubelaid A, Belkhier Y (2025) Energy management in networked microgrids: A comparative study of hierarchical deep learning and predictive analytics techniques. *Energy Convers Manage X* 25: 100828. https://doi.org/10.1016/j.ecmx.2024.100828
23. Saranya M, Samuel GG (2024) Energy management in hybrid photovoltaic-wind system using optimized neural network. *Electr Eng* 106: 475–492. https://doi.org/10.1007/s00202-023-01991-4
24. El Mezdi K, El Magri A, El Myasse I, et al. (2023) Performance improvement through nonlinear control design and power management of a grid-connected wind-battery hybrid energy storage system. *Results Eng* 20: 101491. https://doi.org/10.1016/j.rineng.2023.101491
25. Abdelghany MB, Al-Durra A, Gao F (2023) A coordinated optimal operation of a grid-connected wind-solar microgrid incorporating hybrid energy storage management systems. *IEEE Trans Sustainable Energy* 15: 39–51. https://doi.org/10.1109/TSTE.2023.3263540
26. Jasim AM, Jasim BH, Baiceanu FC, et al. (2023) Optimized sizing of energy management system for off-grid hybrid solar/wind/battery/biogasifier/diesel microgrid system. *Math* 11: 1248. https://doi.org/10.3390/math11051248
27. Molu RJJ, Naoussi SRD, Wira P, et al. (2023) Optimization-based energy management system for grid-connected photovoltaic/battery microgrids under uncertainty. *Case Stud Chem Environ Eng* 8: 100464. https://doi.org/10.1016/j.cscee.2023.100464

28. Hemmati R, Faraji H, Beigvand NY (2022) Multi objective control scheme on DFIG wind turbine integrated with energy storage system and FACTS devices: Steady-state and transient operation improvement. *Int J Electr Power Energy Syst* 135: 107519. https://doi.org/10.1016/j.ijepes.2021.107519
29. Oraa I, Samanes J, Lopez J, et al. (2022) Modeling of a droop-controlled grid-connected DFIG wind turbine. *IEEE Access* 10: 6966–6977. https://doi.org/10.1109/ACCESS.2022.3142734
30. Rekioua D, Mokrani Z, Kakouche K, et al. (2023) Optimization and intelligent power management control for an autonomous hybrid wind turbine photovoltaic diesel generator with batteries. *Sci Rep* 13: 21830. https://doi.org/10.1038/s41598-023-49067-4
31. Niveditha N, Singaravel MR (2024) Optimal sizing of PV-Wind generators with a smart EV charging framework to build grid friendly Net Zero Energy Campus. *Sustainable Cities Soc* 111: 105575. https://doi.org/10.1016/j.scs.2024.105575

AIMS Press